Talanta 82 (2010) 502–507

Contents lists available at ScienceDirect

Talanta

journal homepage: www.elsevier.com/locate/talanta

Potentiometric sensor using sub-micron Cu_2O-doped RuO_2 sensing electrode with improved antifouling resistance

Serge Zhuiykov[a,*], Eugene Kats[a], Donavan Marney[b]

[a] Commonwealth Scientific Industrial Research Organisation (C.S.I.R.O.), Materials Science and Engineering Division, 37 Graham Road, Highett, VIC 3190, Australia
[b] Commonwealth Scientific Industrial Research Organisation (C.S.I.R.O.), Land and Water Division, 37 Graham Road, Highett, VIC 3190, Australia

ARTICLE INFO

Article history:
Received 8 April 2010
Received in revised form 28 April 2010
Accepted 30 April 2010
Available online 11 May 2010

Keywords:
Cu_2O–RuO_2
Water quality sensors
Dissolved oxygen
Thin films

ABSTRACT

A Cu_2O-doped RuO_2 sensing electrode (SE) for potentiometric detection of dissolved oxygen (DO) was prepared and its structure and electrochemical properties were analyzed by scanning electron microscopy (SEM), X-ray diffraction (XRD), X-ray photoelectron microscopy (XPS) and energy-dispersive spectroscopy (EDS) techniques. Cu_2O-RuO_2-SE displayed a linear DO response from 0.5 to 8.0 ppm (log[O_2], −4.73 to −3.59) within a temperature range of 9–30 °C. The maximum sensitivity of −47.4 mV/decade at 7.27 pH was achieved at 10 mol% Cu_2O. Experimental evaluation of the Cu_2O-doped RuO_2-SE demonstrated that the doping of RuO_2 not only improves its structure but also enhances both sensor's selectivity and antifouling properties. Selectivity measurements revealed that 10 mol% Cu_2O-doped RuO_2-SE is insensitive to the presence of Na^+, Mg^{2+}, K^+, Ca^{2+}, NO_3^-, PO_4^{2-} and SO_4^{2-} ions in the solution in the concentration range of 10^{-7}–10^{-1} mol/l.

1. Introduction

Electrochemical sensors using semiconductor metal oxide film-SE (MnO_2, Ta_2O_5, Sb_2O_3, IrO_2, TiO_2, RuO_2, ZrO_2 and Co_2O_3) have found wide applications as instruments monitoring various parameters of water quality [1–4]. Among these oxides RuO_2 is a mixed electronic and ionic conductor, having an oxygen defect stoichiometry, which can be utilized for DO measurement in water. Analyzing DO in fresh and/or recycled water is one of the central parameters related to the water quality monitoring. The use of RuO_2 as a promising candidate for SE of the ceramic pH sensor was reported for the first time in 1984 [5]. Since then research of the chemical and electrochemical properties of this material and its modifications has been expanded. So far, the development of highly sensitive electrochemical DO sensors based on RuO_2-SE has unveiled that DO concentration in water can be controlled from 0.5 to 8.0 ppm displaying the Nernstian slope of −41 mV/decade [6,7]. Martinez-Manez et al. [8] also reported −45 mV/decade for non-coated RuO_2-SE, where the discrepancy could be explained by the reported changes of the slope per decade in the pH 7.0–10.0 range [9]. Furthermore, it could be also due to the other redox reactions at the RuO_2 surface, which affect the measured *emf* [10]. Sensitivity, selectivity and bio-fouling resistance (i.e. stability) are the most important properties of water quality sensors. In order to improve them, microstructure control by preparing the nanostructured thin films and doping with noble metal components are known to be very effective [7,11].

Employing small concentration of another nanostructured oxide as a dopant to RuO_2-SE has been considered as a further alternative to the improvement of the semiconductor-SE properties [12,13]. Defect disorder of the doped oxide-SE has usually led to the formation of donor levels located in the upper part of the energy gap of the semiconductor-SE. These donor levels are primarily responsible for the observed improvement in properties [14]. The empirical exploration of mixing RuO_2 and other semiconductors may not only lead to new improved sensing properties but can also enhance the sensor's selectivity and antifouling resistance. However, most of the previous attempts at tailoring RuO_2 by Co_3O_4 [2], TiO_2 [15–17], Ta_2O_5 [18,19], ZrO_2 [20], NiO [21], CeO_2 [22] and La_2O_3 [23] have proved that it was not possible to predict the exact electro-catalytic behaviour of the composite semiconductor-SE. Nevertheless, it was clearly concluded from these studies that the activity in doped RuO_2 heterostructures differs from that of the un-doped RuO_2 [24]. Specifically, the aim of mixing RuO_2 with TiO_2 was to prevent corrosion (or oxidation) of the RuO_2 to RuO_4 or RuO_4^{2-} [16]. Although the improvement of the RuO_2 heterostructure's insensibility to Li^+, Na^+ and Ca^+ ions in the solution has been achieved at the TiO_2-doped RuO_2 at 30 mol% of the doping concentration, there were no reported progress in pH sensitivity [17]. Both studies of RuO_2 doped with Co_3O_4 [2] and NiO [21] suggested that the increase of the dopant content up to 20 mol% leads to an increase of the material's activity towards oxygen evolution. However, the available

* Corresponding author. Tel.: +61 (0)3 9252 6236; fax: +61 (0)3 9252 6246.
E-mail address: serge.zhuiykov@csiro.au (S. Zhuiykov).

0039-9140/$ – see front matter © 2010 Elsevier B.V. All rights reserved.
doi:10.1016/j.talanta.2010.04.066

data were insufficient to outline the trend conclusively and current progress of using these data is slow owing to the lack of knowledge about the actual structure at the functional-group level. In regard to the use of nanostructured RuO_2 for the sensor applications, the situation is even worse since the most of cited studies were simply focused on the catalytic activity of oxygen, and not on the electrochemical behaviour of the doped RuO_2-SE. It has to be understood that the comprehensive characterisation of the doped RuO_2 heterostructure, including a combination of the diffraction, microscopic, spectroscopic and electrochemical measurement methods, needs to be done in an attempt to elucidate the nature of the active sites of RuO_2 heterostructures for DO measurement.

Herein, we present for the first time the performance of the Cu_2O-doped RuO_2-SE in potentiometric DO sensor with such enhanced properties as sensitivity, selectivity and antifouling resistance. Specifically, this paper extends the previous studies of doping RuO_2-SE by combining the results of XRD, XPS, SEM, EDS measurements as well as characterisation of the Cu_2O-doped RuO_2-SE behaviour in the different aqueous solutions. The present work could be described as a tangible step forward in the development of water quality sensors with improved properties of oxide-SE.

2. Experimental

The Cu_2O-doped RuO_2-SE was synthesized on an alumina sensor substrate by the method described elsewhere [7]. In brief, RuO_2 nanoparticles in average size of *ca.* 360 nm were pre-treated at 1000 °C for 2 h in air in order to achieve structure stabilization [6]. The average size of used Cu_2O nanoparticles was *ca.* 46 nm. Cu_2O-doped RuO_2-SEs were made from nanosized chemicals supplied by ABCR GmbH & Co. and Sigma–Aldrich Australia Pty. Ltd., respectively. The alumina sensor substrates were manufactured by Taylor Ceramic Engineering Pty. Ltd., Australia. Platinum (Pt) current conductors of *ca.* 5 μm thick were applied onto the alumina sensor substrate and were sintered at 1000 °C for 1 h in air prior to SE deposition. Then, RuO_2 and Cu_2O nanoparticles were mixed together at the different molar ratio and applied to the platinised alumina substrate using α-terpineol ($C_{10}H_{18}O$, 99.0%) as the carrier. The content of Cu_2O in RuO_2-SE varied from 5 to 25 mol%. The prepared Cu_2O-doped RuO_2-SEs were sintered in two steps: heating to 400 °C at rate of 65 °C/h and stabilization at 400 °C for 2 h before further heating to 800 °C at rate of 100 °C/h in air thereby ensuring the development of nanostructured Cu_2O-doped RuO_2-SEs [7]. The glazing protective layer was applied onto alumina sensor substrates at the final stage of sensor preparation covering both sides of substrates except the active areas of SEs. The protective layer was subsequently sintered at 600 °C for 10 min. Separate standard Ag/AgCl, Cl^- reference electrode was used for both pH and DO measurements. The particle size distribution and surface morphology of the RuO_2 and Cu_2O nanoparticles within the Cu_2O-doped RuO_2-SEs was characterized by FE-SEM (JEOL JSM-6340F) and their composition was subsequently analyzed by a Wet-SEM (HITACHI, S-3000N). EDS measurements were done on LinkISIS manufactured by Oxford Instruments. The results of the X-ray photoelectron spectroscopy (XPS; AXIS-165, Shimadzu/Kratos, Japan) were performed using a monochromatic aluminium X-ray source (1386.6 eV) operating at 15 kV and 7 mA under ultra-high vacuum (10^{-5} Pa). The carbon peak at 284.2 eV was used as a reference to estimate the electrical charge effect. A Bruker D8 Advance X-ray Diffractometer with CuKα (with wavelengths $K\alpha_1$ λ = 1.5406 Å, $K\alpha_2$ λ = 1.54439 Å with a $K\alpha_2$ ratio of 0.5) radiation operating at 40 kV, 40 mA and monochromatised with a graphite monochromator was employed to determine the XRD patterns. XRD intensity and record was collected using a scintillation detector. Each sample was scanned over the 2θ range of 15–85° with a step size of 0.02° and a count time of 4 s per step.

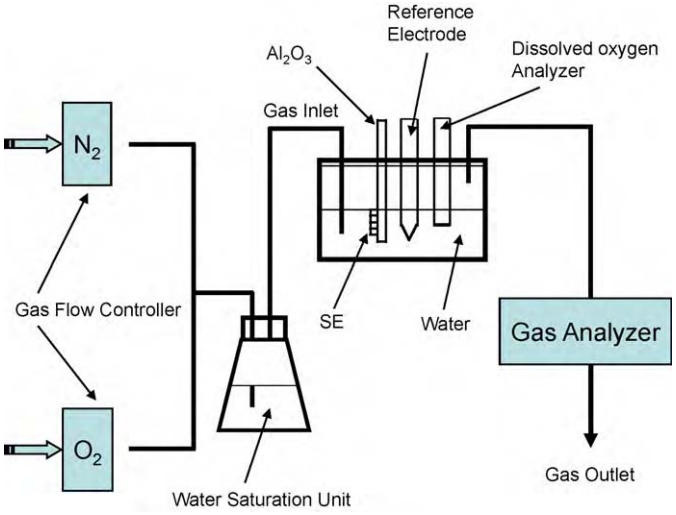

Fig. 1. Simplified schematic view of the experimental setup used in electrochemical DO measurements.

Analyses were performed on the collected XRD data for the sample using the Bruker XRD search match program EVA™. Crystalline phases were identified using the ICDD-JCPDS powder diffraction database.

Sensing properties of the different Cu_2O-doped RuO_2-SEs were analyzed by utilizing sensors in a conventional water-flow apparatus equipped with a heating facility. A typical experimental setup for DO measurements is presented in Fig. 1.

The experimental setup enables open-circuit potentials of up to three electrodes to be collected simultaneously under various predetermined $p(O_2)$ and temperatures. The *emf* of the sensor was monitored by a Keithley 2010 electrometer with a high-input impedance (>10^9 Ω), which was connected to a PC. The temperature was carefully measured by a K-type thermocouple located adjacent to the sensor. The pH sensing performance was tested in stirring water at different temperatures, where the pH changes were prepared by acid–base titration. The dynamic range of this method is from 2.0 to 13.0 pH. The temperature of the solution ranged from 9 to 35 °C. A commercial pH meter (HANNA Instruments, USA), calibrated daily using pH 4.0 and 7.0 buffer solutions was used to monitor the pH of the solution. To test the response behaviour of the DO sensor, the potential response of the sensor as a function of DO concentration of a test solution ranging from 0.5 to 8.0 ppm was measured. A commercial dissolved oxygen analyser with auto-calibration function (HI-9142, HANNA Instruments, USA) was employed to measure DO concentrations against the measured *emf* of the Cu_2O-doped RuO_2-SEs. The analyzer was calibrated before each measurement. The electrochemical characteristics of thin-film ceramic sensors in terms of sensitivity, selectivity, limit of detection and working concentration interval were studied by means of potentiometric measurements. The sensor response to a number of dissolved salts (KCl, Li_2SO_4, Na_2SO_4, $Mg(NO_3)_2$, $Ca(NO_3)_2$ and Na_2HPO_4) was investigated over concentration ranges from 10^{-7} to 10^{-1} mol/l. The individual solutions in the concentration range of 10^{-7}–10^{-2} mol/l were prepared by successive 10-fold dilution of the corresponding stock solutions of 10^{-1} mol/l.

3. Results and discussion

Fig. 2 shows patterns of the sub-micron Cu_2O-doped RuO_2-SE sintered on the alumina sensor substrate. Analysis of the diffraction peaks for RuO_2 illustrate that they can be indexed to the tetragonal structure of RuO_2 with a space group of *P*42. Diffraction

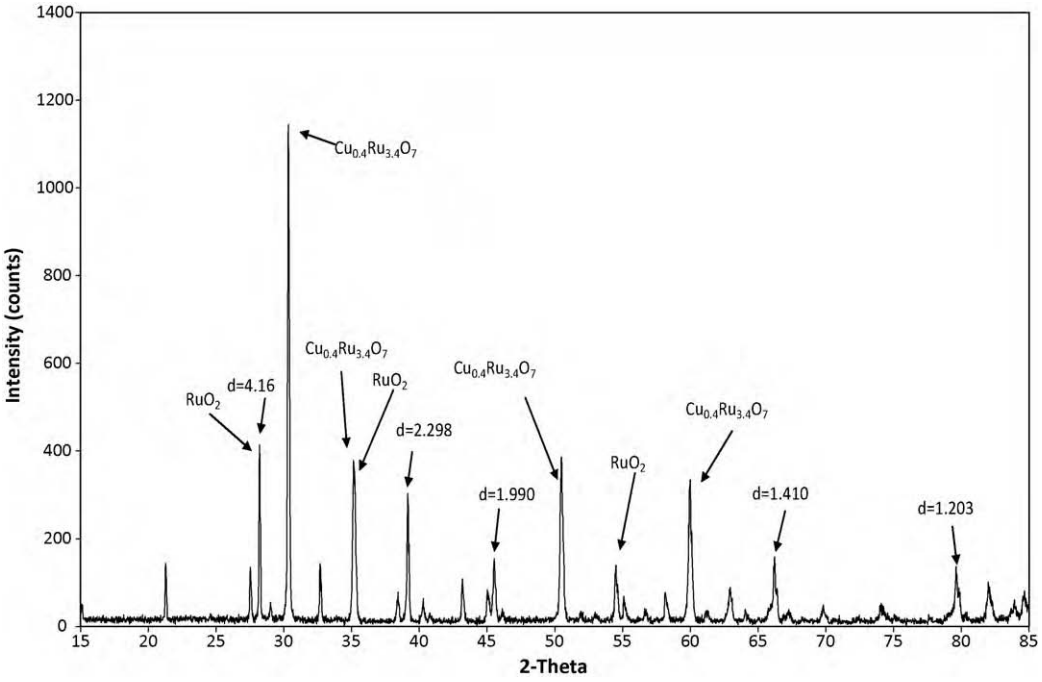

Fig. 2. XRD patterns of the sub-micron Cu_2O-doped RuO_2-SE of the electrochemical DO sensor.

peaks for cubic phase of the copper ruthenium oxide $Cu_{0.4}Ru_{3.4}O_7$ with a space group *I*23 has also been indexed. All well-developed diffraction peaks were narrow indicating that ruthenium oxide and copper ruthenium oxide structures are of good crystallinity. In addition, few alumina peaks were detected. However, their intensity was rather low. This result indicates that both $Cu_{0.4}Ru_{3.4}O_7$ and RuO_2 are thermally stable even at high sintering temperature (800 °C) without additional phase change, formation of any solid solution with alumina, decomposition and evaporation.

EDS measurements of each of the different 10 mol% Cu_2O-doped RuO_2-SE showed the presence of all relevant peaks. Their intensities were different. Ru, Cu and O peaks were clearly identified, as illustrated in Fig. 3A. In addition, weak Al peak representing alumina sensor substrate was also observed. Fig. 3B shows SEM image of the surface of 10 mol% Cu_2O-doped RuO_2-SE with size of the grains measurement. It is seen that the surface of Cu_2O-doped RuO_2-SE has no open porosity compared to the relatively porous structure

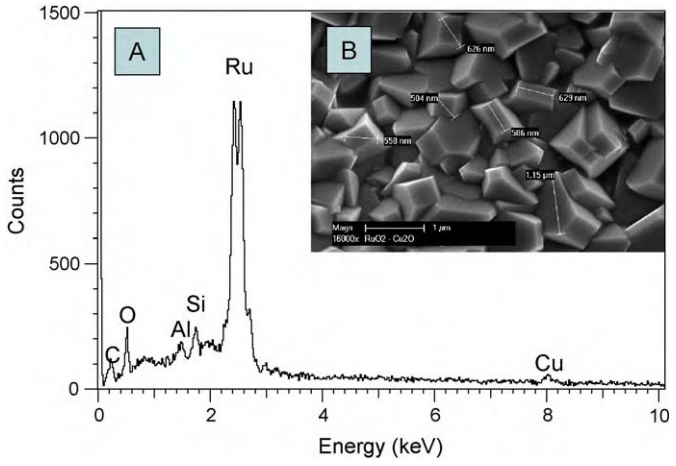

Fig. 3. EDS measurements of 10 mol% Cu_2O-doped RuO_2-SE (A); SEM image of the surface morphology with dimensions of the main grains of Cu_2O-doped RuO_2-SE (B).

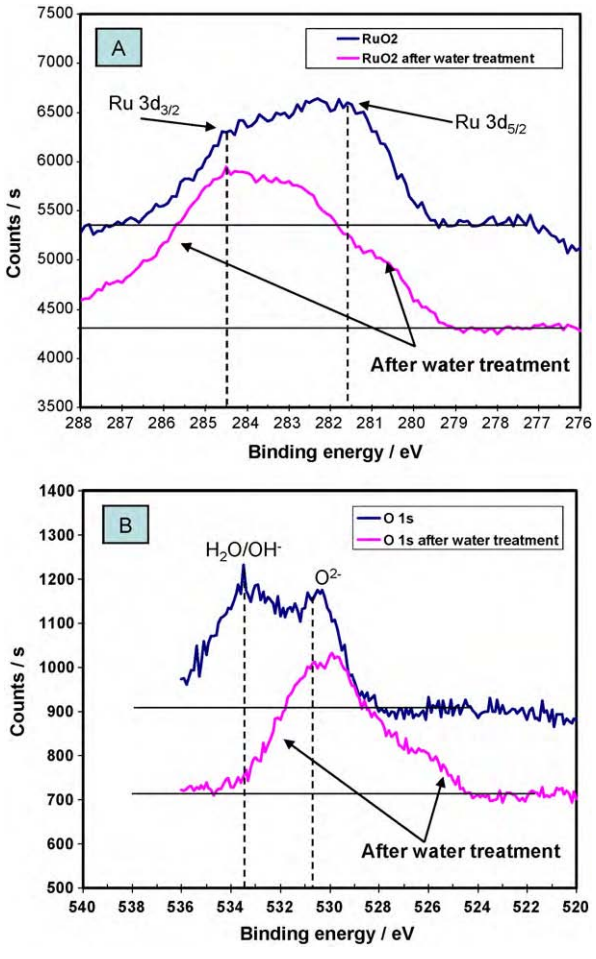

Fig. 4. XPS core level photoelectron peaks for Ru 3d (A) and O 1s (B).

of the reported RuO_2-SE [3,6]. All Cu_2O-doped RuO_2 grains were homogeneously distributed on the surface of the SE. The average detected grain size was in the range of 500–600 nm. These results suggest that the Cu_2O doping of RuO_2 decreases both open and bulk porosity as well as develops high surface-to-volume ratio important for high sensitivity of the sensor.

Qualitative XPS analysis of the Cu_2O-doped RuO_2-SEs was performed, with the typical survey and high-resolution spectra shown in Fig. 4. Analysis of data collected from the general XPS spectrum recorded for freshly deposited Cu_2O-doped RuO_2-SE onto the alumina substrate and for the same SE after 23 days in water indicated that the surface of SE is clean and free from pronounced amounts of contaminant except for carbon. XPS measurements typically gives a compositional data for the surface layers (30–50 Å) corresponding to the penetration depth of the soft X-rays into the sample. Surface analysis of the sample is usually complicated by the presence of overlapping peaks. In our case Ru 3d levels are obscured by the C 1s level. The data therefore were quantified by using the instrument's peak-fitting program for analysis in order to fit Ru $3d_{5/2}$ level alongside the C 1s peak.

The XPS surface atomic ratio was calculated with the integrated intensity of the Ru $3d_{5/2}$ and Ru $3d_{3/2}$ peaks. They display the characteristic shape of core level spectra for Ru 3d and O 1s, presented in Fig. 4A and B, respectively. The Ru 3d core level spectrum is characterized by a pair of relatively narrow peaks corresponding to the 5/2 and 3/2 spin–orbit components located at 284.5 and 281.6 eV, respectively. The 2.9 eV separation between both peaks is different to the previously published value of 4.1 eV for un-doped RuO_2 [25]. There is also no discernable feature at 284.6 eV, where C 1s core level peak of adventitious carbon contamination is expected, indicating that the level of contamination is relatively low. However, after exposure to water for 23 days, the shape of the peak for Ru 3d has altered suggesting a major change in the electronic structure of SE. In particular, the sensor's behaviour at further pH measurements indicated that pH-drift was attributed to the variations of the Ru(IV)/Ru(III) ratio in the SE in accordance with the following reaction [9]:

$$2RuO_2 + 2H_{ag}^{+} + 2e^{-} \leftrightarrow Ru_2O_3 + H_2O. \quad (1)$$

This behaviour is in a sharp contrast with that of RuO_2 electrodes prepared by the thermal decomposition of 0.3 M $RuCl_3$ aqueous solution, where polarization of RuO_2 electrode causes no substantial transformations in the core level spectra for Ru 3d and O 1s regions [25]. This discrepancy clearly points to the fact that structural water molecules in RuO_2 play a crucial role in determining the relative stability of the oxide towards reduction.

The O 1s region was decomposed into two contributions: metal–O (530.8 eV) in the metal oxide and metal–OH (533.4 eV). The area ratio of metal–OH/metal–O in the O 1s peaks were distinguishably decreased in the same sample exposed to the water for 23 days, when compared with the freshly prepared sample. This observation also confirms that the oxygen signal results from the reaction of ruthenium metal with molecular oxygen rather than with traces of other molecules dissolved in water. In fact three components have been used to fit the O 1s core level peak of as-prepared RuO_2 (Fig. 4B). Component (I) at lower binding energy (530.8 eV) is attributed to O^{2-} (oxygen bound to ruthenium). Components (II) and (III) at 532.0 and 533.4 eV are attributed to OH^{-} and H_2O adsorbed at the surface of RuO_2. This was a significant decrease of components (II) and (III) upon exposure of the electrode to the water for 23 days, confirming partial oxidation of Ru(IV) to Ru(III) in the SE discussed elsewhere [9].

The sensing performance of the devices using different Cu_2O-doped RuO_2-SEs revealed that the sensor's DO sensitivity depends on the percentage of Cu_2O in RuO_2-SE. The *emf* response to the changes of DO concentration from 0.5 to 8.0 ppm ($\log[O_2]$, −4.73 to −3.59) in water for the sensors using different Cu_2O-doped RuO_2-SEs is shown in Fig. 5A. The *emf* values were almost linear to the logarithm of DO concentration at a water temperature of 21 °C. Similar characteristics were also obtained for all temperatures examined within the working temperature range of 9–30 °C. Fig. 5B summarizes the experimental sensitivity values of the sensors for each Cu_2O-doped RuO_2-SE. It is apparent that the percentage of Cu_2O dopant in RuO_2 influences the DO sensitivity of the sensor in a quite complicated manner. Two distinguished maxima in DO sensitivity have been found for 10 mol% and 20 mol% of Cu_2O in RuO_2-SE, respectively. Maximum of the Nernstian slope of −47.4 mV/decade has been obtained for 10 mol% of Cu_2O in RuO_2-SE. It was higher than those previously published results of −41 mV/decade [6] and −45 mV/decade [8] for RuO_2-SE. Moreover, DO sensor using 10 mol% of Cu_2O-doped RuO_2-SE was capable of detecting even lower DO concentration of 0.5 ppm that was not possible for sensors based on RuO_2-SEs [6]. Consequently, all following tests were performed on sensor using 10 mol% Cu_2O-doped RuO_2-SE.

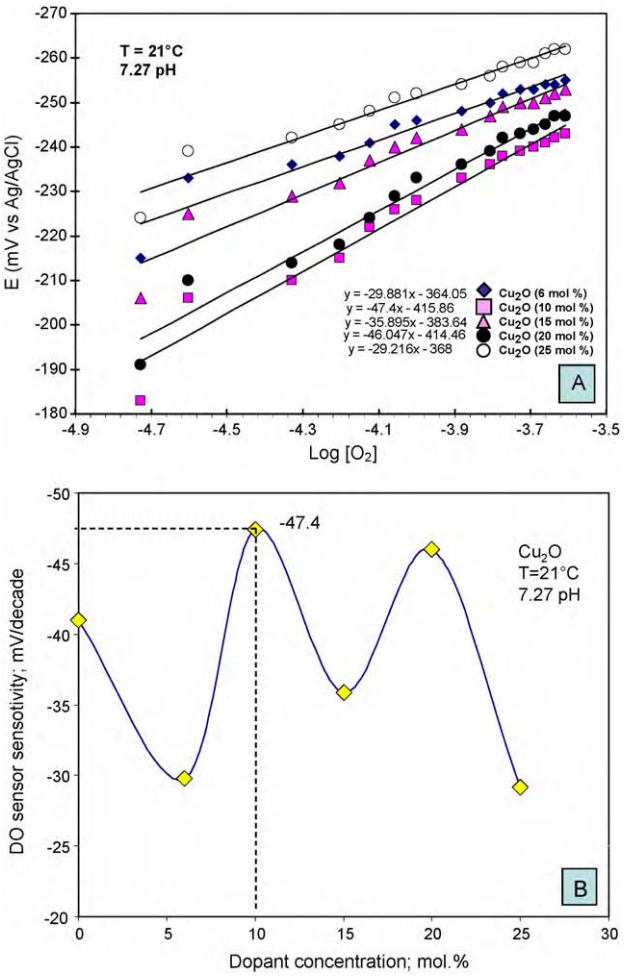

Fig. 5. (A) *Emf* variations for Cu_2O dopant concentration in RuO_2-SE vs. DO measured at a water temperature of 21 °C; (B) measured DO sensor sensitivity vs. percentage of the Cu_2O dopant in RuO_2-SE.

Further DO testing (0.5–8.0 ppm) at three different pH values indicated that as the pH of the solution changes toward either more acidic or more alkaline values, the DO sensitivity decreases, as shown in Fig. 6. It decreases from the maximum of −47.4 mV/decade at pH 7.27 down to −25.5 mV/decade at pH 5.32 and −17.2 mV/decade at pH 9.0. The results obtained in alkaline solutions also revealed that as pH of the solution increases to

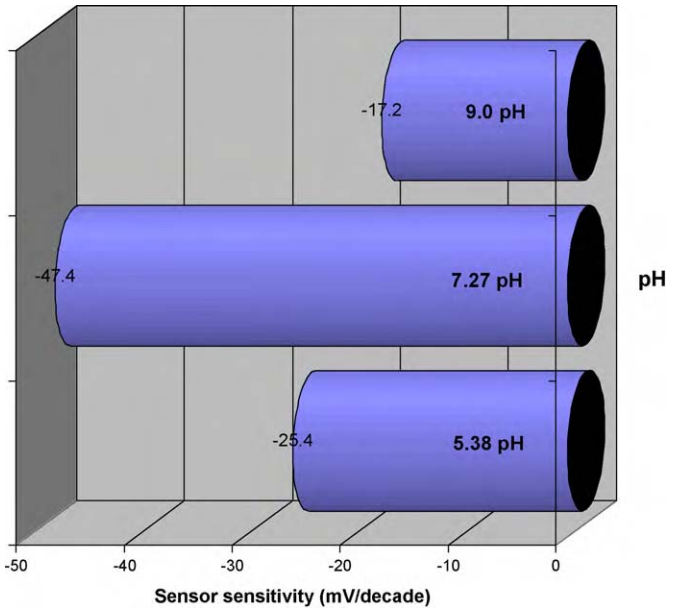

Fig. 6. DO sensitivity of the sensor using 10 mol% Cu_2O-doped RuO_2-SE vs. pH changes of the solution.

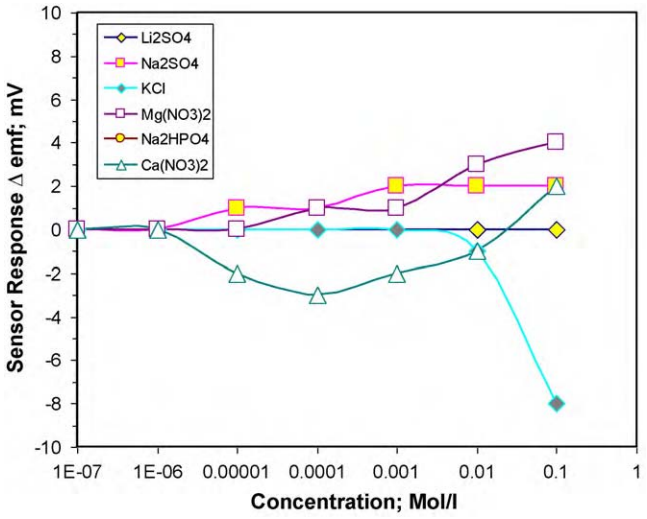

Fig. 7. Selectivity of DO sensor based on sub-micron Cu_2O-doped RuO_2-SE.

~9.0 pH the response/recovery rate becomes faster stabilizing more quickly depending upon the solution alkalinity. This behaviour indicated that both OH^- and O_2^- ions act to accelerate the surface-forming process and possibly are directly involved through, for example, the heterogeneous dissolution of the sub-micron RuO_2-SE according to [10]:

$$RuO_2 + 4OH^- \leftrightarrow RuO_4^{2-} + 2H_2O + 2e^- \quad (2)$$

$$RuO_2 + O_2^- \leftrightarrow RuO_4 + e^- \quad (3)$$

This explains the observed decrease in the degree of surface oxidation with increasing pH of the solution [26]. Both reactions (2) and (3) also indicate that, as pH of the solution getting more alkaline (9.0 pH) or more acidic (5.0 pH), a Faradaic oxygen reduction reaction becomes not only a one-electron process but rather a mixed-potential multi-step process [9]. In general the higher oxidation states of transitional metal ions are much more stable at higher pH values, but in case of RuO_2 it is possible that unstable hydroxyl-ruthenate complexes are formed in accordance with reaction (2) [10]. The stability of these complexes on the surface is probably less in acid solution due to protonation effects [27]. Therefore the maximum DO sensitivity can be achieved at the neutral pH.

Further interesting observations were made during the testing of the 10 mol% Cu_2O_3-doped RuO_2-SE for selectivity measurement. As the analyzed liquid media in most cases represent multi-component systems, the problem of inadequate selectivity under direct potentiometric measurement arises. Thus, the investigation of interfering effects of various dissolved ions on the sensor measuring potential in aqueous solutions has been carried out by the method of fixed interference. It was found that during selectivity measurements the sensor based on 10 mol% Cu_2O-doped RuO_2-SE is insensitive to the presence of Na^+, Mg^{2+}, K^+, Ca^{2+}, NO_3^-, PO_4^{2-} and SO_4^{2-} ions in the solution in the concentration range of 10^{-7}–10^{-1} mol/l. The sensor was also almost insensitive to the presence of Cl^- ions in the solution in the concentration range of 10^{-7}–10^{-2} mol/l. Only when the Cl^- concentration in the test solution increased to 10^{-1} mol/l the sensor's *emf* exhibited substantial changes as clearly presented in Fig. 7. In this figure Δemf is the difference between measurements before and after injection of the appropriate concentration of dissolved salt into the test solution. It was found that 10 mol% Cu_2O-doped RuO_2-SE is insensitive to the presence of both Li_2SO_4 and Na_2HPO_4 within the whole measured concentration range of 10^{-7}–10^{-1} mol/l. Consequently, the experimental selectivity results in Fig. 7 for Li_2SO_4 and Na_2HPO_4 have been overlapped.

Long-term stability trial has been organized on the Karkarook Park Lake, Australia for sensors attached with RuO_2-SE and 10 mol% Cu_2O-doped RuO_2-SE at the end of 2009. Fig. 8 exhibits SEM images of both RuO_2-SE and 10 mol% Cu_2O-doped RuO_2-SE after their testing in Karkarook Park Lake for 3 months. The *emf* responses of the sensors based on the above SE did not change during the first 3 months. It is evident from these SEM images that the bio-fouling has

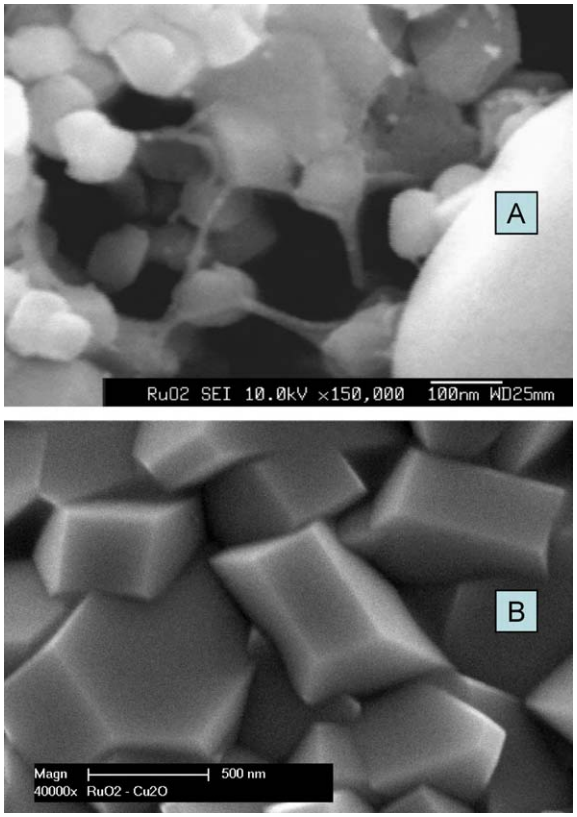

Fig. 8. SEM images of the surface of RuO_2-SE (A) and 10 mol% Cu_2O-doped RuO_2-SE (B) after their testing in Karkarook Park Lake for 3 months.

already started accumulating on the RuO_2 grains (Fig. 8A), whereas no traces of bio-fouling has been identified on the Cu_2O-doped RuO_2-SE (Fig. 8B). Cu_2O has been known as an effective antifouling pigment in the chemically active paint systems for marine vessels [28]. It is not lipophilic and shows only a slight tendency for bioaccumulation [29]. In the presence of DO, copper complexes are oxidized to Cu^{2+}, which is the main biocidal species formed from Cu_2O. Long-term antifouling resistance testing is currently in progress with initial results looking encouraging. These results confirmed that the improvement in antifouling resistance of the RuO_2-SE was attributed to the presence of Cu_2O in its structure.

All the above results appear to suggest that the potentiometric DO sensor based on Cu_2O-doped RuO_2-SE can be utilized as an effective measuring tool for analysis and control of DO level of complex aqueous media. Extending sensitivity and selectivity properties of these water quality sensors might yield a further utilization of these new sensitive ceramic semiconductor materials.

4. Conclusions

The morphology, surface composition and sensing properties of the Cu_2O-doped RuO_2-SE of the potentiometric DO sensor was studied for the freshly prepared SE before and after its exposure to water for 23 consecutive days. It was unveiled that the doping of the RuO_2-SE by Cu_2O has been demonstrated as one of the effective way for improving both antifouling resistance and sensing properties of the electrochemical DO sensor. XPS data also revealed that the introduction of Cu_2O into RuO_2 does not lead to a significant change in the Ru chemical state (Ru $3d_{5/2}$). The results obtained suggest that the use of a low concentration of doping oxide in the base oxide is a useful way to improve the sensing characteristics of water sensors. The presented thin-film electrochemical DO sensors with improved antifouling resistance have been shown to be a prospective tool for the assessment of water quality. Utilising new doped chemically sensitive semiconductor materials as the SE of these sensors will also allow extension of both the sensitivity and selectivity properties of the all solid-state thin-film micro-sensors, and consequently, the scope of problems solved by advanced materials science.

Acknowledgements

This work was partially supported by Research and Development Program of CSIRO Sensors and Sensor Networks Transformation Capability Platform and CSIRO Materials Science and Engineering Division – strategic co-investment project “Water Quality Sensors”. The help from the Prof. Miura’s laboratory of KASTEC, Kyushu University, Japan in regard to preparation and testing some of the SE samples has been appreciated.

References

[1] C. Arnold, D. Haerinher, I. Kiselev, J. Goschnick, Sens. Actuators B: Chem. 116 (2006) 90.
[2] K. Macounova, M. Makarova, J. Jirkovsky, J. Franc, P. Krtil, Electrochim. Acta 53 (2008) 2656.
[3] S. Zhuiykov, D. O’Brien, M. Best, Meas. Sci. Technol. 20 (2009) 095201.
[4] E. El-Deen, M. El-Giar, D.O. Wopf, J. Electroanal. Chem. 609 (2007) 147.
[5] A. Fog, R.P. Buck, Sens. Actuators B: Chem. 5 (1984) 137.
[6] S. Zhuiykov, Electrochem. Commun. 10 (2008) 839.
[7] S. Zhuiykov, Sens. Actuators B: Chem. 136 (2009) 248.
[8] R. Martinez-Manez, J. Soto, J. Lizondo-Sabater, E. Garcia-Breijo, L. Gil, J. Ibanez, I. Alcaina, S. Alvarez, Sens. Actuators B: Chem. 101 (2004) 295.
[9] S. Zhuiykov, Ionics 15 (2009) 693.
[10] P. Kurzweil, J. Power Sources 190 (2009) 189.
[11] S. Zhuiykov, Sens. Actuators B: Chem. 129 (2008) 431.
[12] J. Ribeiro, F.L.S. Purgato, K.B. Kokoh, J.M. Leger, A.R. de Andrade, Electrochim. Acta 51 (2008) 98.
[13] J. Rossmeisl, Z.W. Qu, H. Zhu, G.J. Kroes, J.K. Norskov, J. Electroanal. Chem. 607 (2007) 83.
[14] J. Nowotny, T. Bak, M.K. Nowotny, L.R. Sheppard, J. Phys. Chem. 111 (2006) 18492.
[15] A. Pintar, J. Batista, T. Tisler, Appl. Catal. B: Environ. 84 (2008) 30.
[16] J.R. Osman, J.A. Crayston, A. Pratt, D.T. Richens, Mater. Chem. Phys. 110 (2008) 256.
[17] L.A. Pocrifka, C. Goncalves, P. Grossi, P.C. Colpa, E.C. Pereira, Sens. Actuators B: Chem. 113 (2006) 1012.
[18] S. Song, H. Zhang, X. Ma, Z. Shao, R.T. Baker, B. Yi, Int. J. Hydrogen Energy 33 (2008) 4955.
[19] J. Ribeiro, M.S. Moats, A.R. de Andrade, J. Appl. Electrochem. 38 (2008) 767.
[20] J. Wang, W. Zhu, X. He, S. Yang, Catal. Commun. 9 (2008) 2163.
[21] K. Macounova, M. Makarova, P. Krtil, Electrochem. Commun. 11 (2009) 1865.
[22] P. Nowakowski, S. Villain, K. Aguir, J. Guerin, A. Kopia, J. Kusinski, F. Guinnetin, J.R. Gavarri, Thin Solid Films 10 (2010) 2801.
[23] S. Zhuiykov, D. Marney, E. Kts, Int. J. Appl. Ceram. Technol., in press.
[24] Y. Takasu, Y. Marakami, Electrochim. Acta 45 (2000) 4135.
[25] D. Rocherfort, P. Dabo, D. Guay, P.M.A. Sherwood, Electrochim. Acta 48 (2003) 4245.
[26] H. Kohler, W. Göpel, Sens. Actuators B: Chem. 4 (1991) 345.
[27] M. Pourbaix, NACE (1974) 644.
[28] D. Szezuka, J. Werner, S. Oswald, G. Berh, K. Wetzing, Appl. Surf. Sci. 179 (2001) 301.
[29] D.M. Yebra, S. Kiil, K. Dam-Johansen, Prog. Org. Coat. 50 (2004) 75.